Available online at www.sciencedirect.com

ScienceDirect

Procedia Structural Integrity 68 (2025) 1031–1037

Structural Integrity Procedia

www.elsevier.com/locate/procedia

European Conference on Fracture 2024

Tuning mechanical response of nonuniform triangular lattice material via graph neural network based inverse design algorithm

Giuseppe Bonfanti[a,b], Federica Buccino[b], Laura Maria Vergani[b], Chao Gao[a]*

[a]*Department of mechanical and industrial engineering, NTNU, Richard Birkelands vei 2B, Trondheim 7491, Norway*
[b]*Department of mechanical engineering, Politecnico di Milano, Via La Masa 1, 20156 Milano, Italy*

Abstract

Strut-based lattice materials with uniform topology have recently received many attentions from scientific and industrial communities because of its exceptional mechanical properties—e.g., high strength-to-weight ratio and energy-absorption-to-weight ratio—and ease of manufacturing. However, many natural strut-based lattice materials show highly nonuniform topology and exhibit much larger design space in terms of linear and nonlinear mechanical behaviors. The exploration of this vast design space is very challenging. Recently, owing to the emergence of deep learning (DL) neural networks, DL-based approach offers great potential to tackle traditional challenges. In this preliminary study, an integrated numerical-DL approach has been developed to tuning the mechanical response of nonuniform strut-based materials. A nonuniform triangular topology was selected to construct strut-based lattice material as an example. Linear elastic material model was employed for each strut of lattice materials. Graph neural network was chosen to build surrogate model to predict global mechanical response—particularly nondimensional effective stiffness, nondimensional effective critical strength, and effective Poisson's ratio—of lattice material. Genetic algorithm was exploited to inversely design nonuniform strut-based lattice materials with optimized properties. The nondimensional effective stiffness, nondimensional effective critical strength, effective Poisson's ratio can be easily tuned in a wide range. Our results demonstrated the feasibility of our integrated approach to design highly nonuniform strut-based lattice materials.

Keywords: Graph Neural Network; Genetic Algorithm; Inverse-Design; Lattice Material; Nonuniform topology;

* Corresponding author. *E-mail address:* chao.gao@ntnu.no

10.1016/j.prostr.2025.06.166

1. Introduction

Lattice material is a lightweight material often constructed by struts, plates, or shells. The architecture of lattice material defines its mechanical response. Due to its high degree of freedom in design and technological advancement in additive manufacturing, lattice material has attracted increasing interest from scientists and engineers since the beginning of this century (Benedetti, du Plessis et al. 2021). For example, by designing the architecture of lattice material rationally, researchers have demonstrated its unique mechanical properties—e.g., ultrahigh strength-to-density ratio (Schaedler, Jacobsen et al. 2011), negative Poisson's ratio (Xue, Lin et al. 2023), and negative stiffness (Ha, Lakes et al. 2019). These extraordinary mechanical properties make lattice material an excellent option for many industrial applications—e.g., aerospace (Najmon, DeHart et al. 2018), biomedical implants (Murr, Gaytan et al. 2010), heat dissipation (Wadley and Queheillalt 2007), energy absorption (Sunder Sharma, Yadav et al. 2022), and filters (Pan, Han et al. 2020). Despite of these attractive properties, lattice material can easily experience catastrophic failure modes—e.g., brittle-like crack propagation under uniaxial tension and buckling under uniaxial compression—because of its uniform architecture, thereby becoming a challenge in wider industrial applications. To tackle this challenge, we and others have recently started to investigate nonuniform lattice material—its nonuniformity can be controlled globally or locally. Lattice material that is carefully designed on its nonuniformity has the potential to obtain enhanced mechanical response—e.g., higher buckling resistance (Maurizi, Gao et al. 2022) and damage tolerance (Gu, Chen et al. 2018).

Given the promising mechanical response of nonuniform lattice materials, there has been surprisingly little study done on the design of nonuniform lattice materials. Three main challenges in design are: (1) *complexity in building a theoretical model to predict the mechanical response of nonuniform lattice material*. Theoretical modeling is a classic design approach for simple uniform lattice material. Despite its advantages in providing faster prediction and a deeper understanding of physical mechanisms, theoretical modeling is very difficult to apply to nonuniform lattice materials because of its complex architecture and stress state. (2) *large parametrical space of nonuniformity lattice material*. Unlike traditional uniform lattice material, nonuniform lattice material has much larger parametrical space. For instance, strut-based lattice material can have nonuniformity in geometrical parameters—e.g., topology, connectivity, strut thickness—and material combinations (Pan, Han et al. 2020). Although large parametrical space produces tunable mechanical properties, it requires a lot of experimental study that is challenging or inconvenient to accomplish. (3) *high computational cost of simulation*. To evaluate the homogenized mechanical response of nonuniform lattice material, a much larger model is required to be built in finite element analysis (Roberts and Garboczi 2002). Moreover, large parametrical space also causes more need to build different models of nonuniform lattice material for simulation. This drawback adds additional time and cost in designing.

More recently, the emergence of deep learning (DL) neural networks has enabled the possibility to develop DL-based design approaches for lattice material. Owing to DL's advantages in a much lower computational cost compared to traditional methods, excellent adaptation to complex structures, and ability to explore the large design space given by the tunable mechanical properties of the nonuniform lattice structure, also due to the lack of human intuition linked to the process, DL-based design approach offers high potential in assessing, designing and predicting mechanical responses of lattice material. Specifically, graph neural network (GNN)—one of the recently developed DL neural networks is developed to process graph-based data—represents strut-based lattice structure by nodes and edges, making GNN an ideal tool to tackle the main challenges of designing nonuniform lattice material. GNN has been preliminarily utilized for the prediction of lattice structure properties, showing its excellent ability to predict lattice materials (Maurizi, Gao et al. 2022, Jiang, Wang et al. 2024).

This paper describes the design of nonuniform triangular strut-based lattice material with tunable mechanical response—specifically, nondimensional effective stiffness, nondimensional effective critical strength, and effective Poisson's ratio. The design method exploits traditional genetic algorithm (GA) and recent GNN; GNN works as a surrogate model to predict the mechanical response of nonuniform strut-based lattice material. The paper is organized as follows: the methods are detailed in Section **Error! Reference source not found.**. The GNN prediction results and GA optimization results are presented and discussed in Section **Error! Reference source not found.**. The conclusions of this work are given in Section **Error! Reference source not found.**.

2. Methods

2.1. Finite Element Simulation

The nonuniform triangular lattice material, as shown in Fig. 1A, has 20 nodes and 43 struts. To construct the dataset of nonuniform triangular lattice material, the initial horizontal coordinates of the nodes are randomly generated by using NumPy library (Harris, Millman et al. 2020) through the function *random.uniform*—function draws samples uniformly distributed over a half-open interval. The initial vertical coordinates of the nodes are fixed. Each set of coordinates is associated with one specific design and a total of 10,000 coordinates set has been created. The geometrical parameters selected for the construction of the dataset are $L_y = 4\,mm$ and $L_x = [2.5,\ 3.5]\,mm$, respectively. The in-plane thickness of rectangular strut was kept as $t_a = 1\,mm$, while the out-of-plane thickness of that was kept as $t_b = 20\,mm$ to avoid the buckling of structure in out-of-plane direction. Linear elastic material model—Young's modulus $E = 1\,GPa$ and Poisson's ratio $\nu = 0.3$—was assigned for struts. All FE models were meshed with 10 quadratic Timoshenko-beams elements per strut after the study of mesh sensitivity has been performed. The structural analysis to determine the critical displacement (δ_{CR}) of structural instability was first solved by ABAQUS/BUCKLE to obtain eigenmodes. By introducing first eigenmode with imperfection, the lattice structure was subjected to a displacement of $\delta_y = 2\delta_{CR}$—displacement that allows the examination of the non-linear response of buckling behavior. The FE results—reaction forces, nodal displacements, and coordinates—were stored as database for training, validation and testing in the deep learning. Commercial FE software ABAQUS 2022 was exploited to perform simulations on a 8-core Intel® Core™ i7-11800H Processor @2.30 GHz PC with 32 GB RAM.

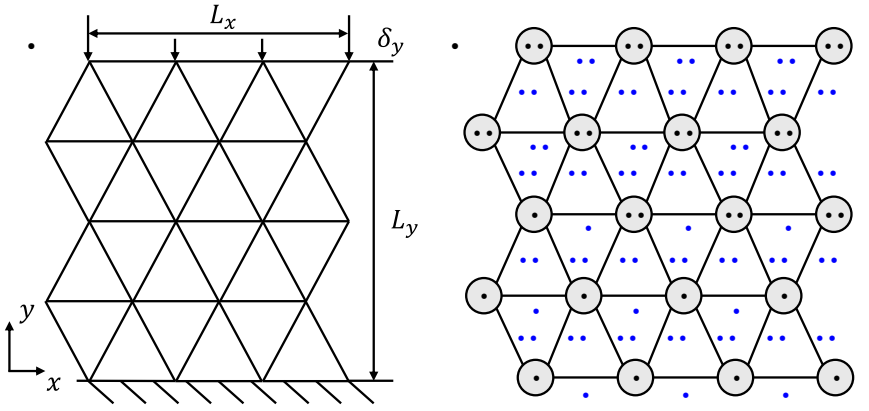

Figure 1 (A) The schematics of nonuniform triangular lattice structure, and (B) its graph representation for deep learning.

The effective stiffness and Poisson's ratio were defined as $\bar{E} = \frac{F/(t_b \cdot L_x)}{\delta_y/L_y}$, $\bar{\nu} = -\frac{\delta_x/L_x}{\delta_y/L_y} = -\frac{\varepsilon_{xx}}{\varepsilon_{yy}}$, respectively. F is the sum of all vertical reaction forces acting on the top nodes; ε_{xx} is the averaged strain in direction x; ε_{yy} is the averaged strain in direction y. Moreover, the critical load σ_y was obtained by choosing the initial slope change of force-displacement curve.

2.2. The architecture of Graph Neural Network

GNN—deep neural network that operates on graph data (Scarselli et al., 2009)—offers potential to represent lattice structure as graph without losing topological information in an efficient way. Graph Attention Network (GAT) (Veličković, Cucurull et al. 2017)—a GNN layer model uses a shared attentional mechanism to compute an attention coefficient that can specify the importance of each node's feature to the others—was exploited in this study. The PyTorch Geometric (Fey and Lenssen 2019) library was employed within the PyTorch framework (Paszke, Gross et al. 2019) to implement deep learning model. The graph were composed of the same nodes and edges as those of the lattice structure ($N_{node} = 20, N_{edge} = 43$), as shown in Fig. 1B. $\epsilon_i^N = (x_i, y_i, \delta_i)$ and $\epsilon_i^E = \left(x_{ij}, y_{ij}, \left|\left|l_{ij}\right|\right|, E_i^{ax}, E_i^b\right)$ are input features for node and edge, respectively. x_i is the x-axis coordinate of the node i; y_i is the y-axis of the node i; and δ_i is the applied displacement on the node i; $x_{ij} = x_i - x_j$ is the distance in x direction between node i and node

j connected by the strut; Similarly, $y_{ij} = y_i - y_j$ is the distance in y direction; $\left|\left|l_{ij}\right|\right| = \sqrt{{x_{ij}}^2 + {y_{ij}}^2}$ is the euclidian norm of distance vectors; $E_i^{ax} = \frac{EA}{\left|\left|l_{ij}\right|\right|}$ is the axial stiffness where E is the Young's modulus and A the area of strut profile; $E_i^b = \frac{EI}{\left|\left|l_{ij}\right|\right|}$ is the bending stiffness where I is the moment of inertia. The FE results—nodal displacement, reaction forces, effective stiffness, effective strength and effective Poisson's ratio—were embedded in an output vector. The edge feature, node feature and ground truth values were normalized using *StandardScaler* function from the sklearn library. The first layer of the multi-head attention mechanism was stabilized using concatenation, while the others GAT layers were performed by averaging because of the loss of sensibility of the GAT final layer (Veličković, Cucurull et al. 2017). The final layer was composed of a pooling layer—global mean pool that returns batch-wise graph-level outputs by averaging node features across the node dimension. To train this networks, Mean Absolute Error (MAE) $= \frac{1}{n}\sum_{i=1}^{n}|y_i - \hat{y}_i|$ was employed as loss function. The Adam optimizer was used with an initial rate of 0.001 for the model predicting effective stiffness and effective Poisson's ratio and 0.0009 for the model predicting the effective strength, respectively. Moreover, the exponential decay γ of the Adam optimizer was kept as 0.95 every epoch for above three models. L2 regularization was adopted to reduce overfitting with a 1 x 10^{-5} weight decay of the prediction of the effective stiffness and effective Poisson's ratio and 2 x 10^{-5} weight decay for the prediction of the effective strength, respectively. Mini-batching was also employed on training and validation dataset. The total number of data was 10000 and the database was split as follows: 60% of training data, 20% of validation data, and 20% of testing data.

2.3. Inverse Design Algorithm

GA—an algorithm is inspired by biological evolution process (Michalewicz and Schoenauer 1996)—is designed to solve problems with multiple solutions and complex search spaces. Inspired by our work (Maurizi, Gao et al. 2022), we developed the inverse design of nonuniform lattice structure by integrating GA as shown in Fig. 2.

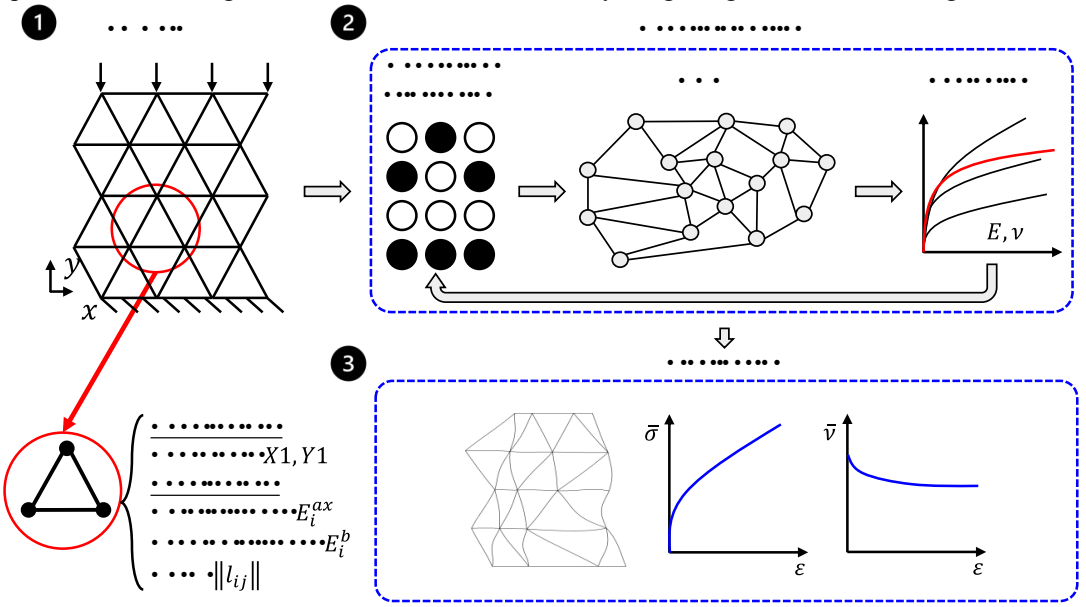

Figure 2 The schematics of inverse design algorithm

The algorithm was run 10 times for each category goal, and GNN's predictions were validated by evaluating the best final designs through FE simulations. The detailed steps to build inverse design algorithm were described as follows.

1) The *random.sample* function from the Python *random* is employed to select an initial population of 100 individuals. This function returns a list of items randomly chosen from the sequence.

2) The previously trained GNN is utilized to assess the fitness of these individuals.
3) Parents are selected using *random.choices* function. The probability of selection is weighted based on the fitness score of each individual. The probabilities are calculated as $p_n = \frac{score_n}{total\ fitness}$, where total fitness is the sum of the N individuals.
4) To generate offspring, a center one-point crossover is used. It results in a child with half of genes from the first parent and half of genes from the second.
5) Offspring is also subject to mutation, and a probability of 0.01 was assigned for each structural node.
6) The offspring's fitness scores are evaluated, and the fitness functions are computed. Subsequently, a comparison is made between the offspring and the parents, considering their fitness scores. Children with higher scores replace parents with lower scores. The fitness function is calculated as $f = f_E + f_\nu \cdot w_\nu + f_{\sigma_y} \cdot w_{\sigma_y}$, where: $f_E = -\left|E_{target} - E_{individual}\right|/E$; $f_\nu = -\left|\upsilon_{target} - \upsilon_{individual}\right|/\nu$; $f_{\sigma_y} = -\left|\sigma_{y_{target}} - \sigma_{y_{individual}}\right|/E$; w_ν is the weight of the Poisson's ratio and w_{σ_y} is the weight of the strength.
7) The iteration of this process repeats over 100 generations.

3. Results

Fig. 3 shows the model performance after the hyperparameters of GNN were carefully tuned. Overall, the model reaches high coefficient of determination R^2—the prediction of nondimensional effective stiffness is $R^2 = 0.984$ (Fig. 3A); the prediction of nondimensional effective strength is $R^2 = 0.946$ (Fig. 3B); and the prediction of effective Poisson's ratio is $R^2 = 0.945$ (Fig. 3C). The prediction of nondimensional effective stiffness reaches the highest R^2. Interestingly, these results show the designed GNN works excellently as a surrogate model to predict different unrelated mechanical properties of nonuniform triangular lattice structure. The strong ability of GNN to process graph-based data ensures that the topological information of nonuniform lattice has been correctly included.

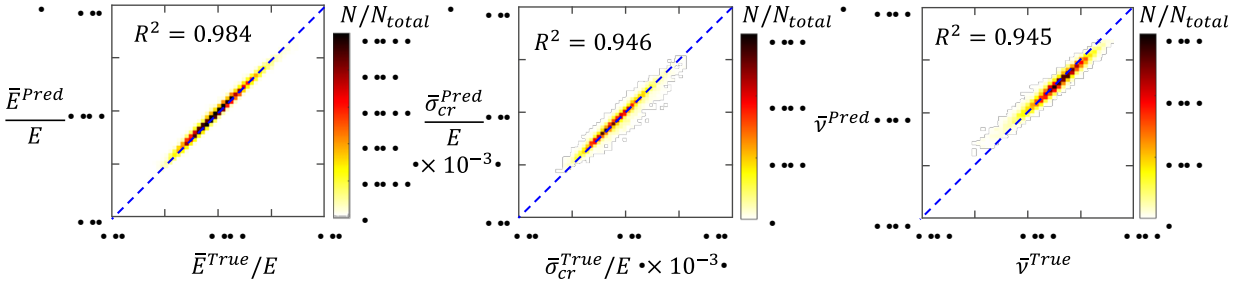

Figure 3 The coefficient of determination R^2 for (A) the prediction of nondimensional effective stiffness, (B) nondimensional effective critical strength, and (C) effective Poisson's ratio by designed GNN.

Fig. 4 shows the results of inverse-designed nonuniform triangular lattice structures and their mechanical properties. Overall, the initial design space of three different mechanical properties has been expanded after the optimization was performed by inverse design algorithm. Specifically, Fig. 4A shows the upper limit of $\bar{E}/E$ increased from ~0.18 to ~0.2 and the upper limit of $\bar{\nu}$ increased from ~0.22 to ~0.26 when the target of inverse design algorithm was set to maximize $\bar{E}/E$ and $\bar{\nu}$, simultaneously. Fig. 4A also shows the lower limit of $\bar{E}/E$ decreased from ~0.12 to ~0.1 and the lower limit of $\bar{\nu}$ decreased from ~0.1 to ~0.02 when the target of inverse design algorithm was set to minimize $\bar{E}/E$ and $\bar{\nu}$, simultaneously. Similarly, Fig. 4B shows the upper limit of $\bar{E}/E$ increased from ~0.18 to ~0.2 and the upper limit of $\bar{\sigma}_{cr}/E$ increased from ~0.003 to ~0.0038 when the target of inverse design algorithm was set to maximize $\bar{E}/E$ and $\bar{\sigma}_{cr}/E$, simultaneously. Fig. 4B also shows the lower limit of $\bar{E}/E$ decreased from ~0.12 to ~0.1 and the lower limit of $\bar{\sigma}_{cr}/E$ decreased from ~0.002 to ~0.0016 when the target of inverse design algorithm was set to minimize $\bar{E}/E$ and $\bar{\sigma}_{cr}/E$, simultaneously. Finally, Fig. 4C shows the upper limit of $\bar{\sigma}_{cr}/E$ increased from ~0.003 to ~0.0034 and the upper limit of $\bar{\nu}$ increased from ~0.22 to ~0.024 when the target of inverse design algorithm was set to maximize $\bar{\sigma}_{cr}/E$ and $\bar{\nu}$, simultaneously. Fig. 4C also shows the lower limit of $\bar{\sigma}_{cr}/E$ decreased from ~0.002 to ~0.0017 and the lower limit of $\bar{\nu}$ decreased from ~0.12 to ~0.04 when the target of inverse design algorithm was set to minimize $\bar{\sigma}_{cr}/E$ and $\bar{\nu}$, simultaneously.

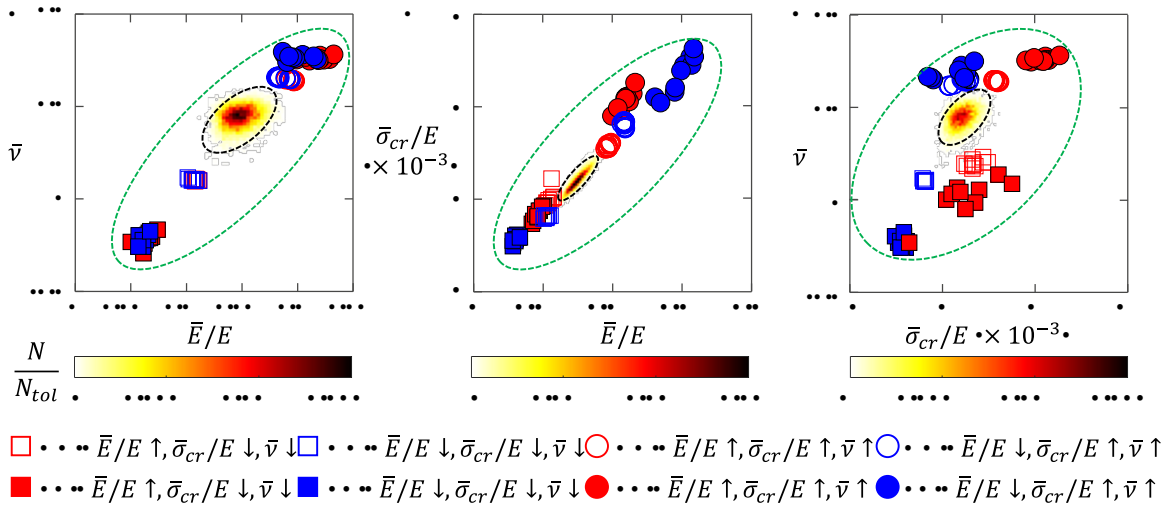

Figure 4 Expanded design space of three different mechanical properties after inverse-design algorithm optimized the design of nonuniform lattice structures. Black dash line represents the initial design space, while green dash line represents the expanded design space.

However, Fig. 4 also shows the discrepancy between GA predicted values and FE simulated results. All solid symbols in Fig. 4 were the results of FE simulations, while all hollow symbols were the values predicted by GA. To investigate the reasons to explain this discrepancy, extensive study has been performed by setting different target values for $\frac{\bar{E}_{target}}{E}, \frac{\bar{\sigma}_{target}}{E}, \bar{\nu}_{target}$, respectively. Fig. 5A shows that the discrepancy between GA predicted and FE simulated $\bar{E}_{obtained}/E$ increases as $\bar{E}_{target}/E$ increases. Interestingly, the discrepancy becomes more significant when $\bar{E}_{target}/E$ is larger than 0.2. It is clearly to demonstrate that GNN, as a surrogate model, can predict the nondimensional effective stiffness of new designs accurately—e.g., $\frac{\bar{E}_{obtained}/E}{\bar{E}_{target}/E} \approx 1.1$ when $\bar{E}_{target}/E$ was set as 0.2—in case the value of nondimensional effective stiffness is inside or close to the range of training dataset. However, the prediction becomes poorer—e.g., $\frac{\bar{E}_{obtained}/E}{\bar{E}_{target}/E} \approx 1.47$ when $\bar{E}_{target}/E$ was set as 0.3—when the nondimensional effective stiffness of new designs are far from the range of training dataset. Similar trend has also been observed in $\bar{\sigma}_{obtained}/E$ (Fig. 5B) and $\bar{\nu}_{obtained}$(Fig. 5C). When the target value of $\bar{\sigma}_{obtained}/E$ and $\bar{\nu}_{obtained}$ is set closer to the range of their training dataset, the prediction accuracy of GA is high—e.g., $\frac{\bar{\sigma}_{obtained}/E}{\bar{\sigma}_{target}/E} \approx 1.05$ when $\bar{\sigma}_{target}/E$ was set as 0.004; $\frac{\bar{\nu}_{obtained}}{\bar{\nu}_{target}} \approx 1.04$ when $\bar{\nu}_{target}$ was set as 0.2. When the target of value of these two nondimensional values is set far from the range of their training dataset, the prediction accuracy of GA is poor—e.g., $\frac{\bar{\sigma}_{obtained}/E}{\bar{\sigma}_{target}/E} \approx$ 1.38 when $\bar{\sigma}_{target}/E$ was set as 0.01; $\frac{\bar{\nu}_{obtained}}{\bar{\nu}_{target}} \approx 1.27$ when $\bar{\nu}_{target}$ was set as 0.5. However, despite the poor prediction accuracy, the inverse design algorithm can successfully build novel lattice materials with enhanced mechanical properties that are beyond the initial range of training dataset.

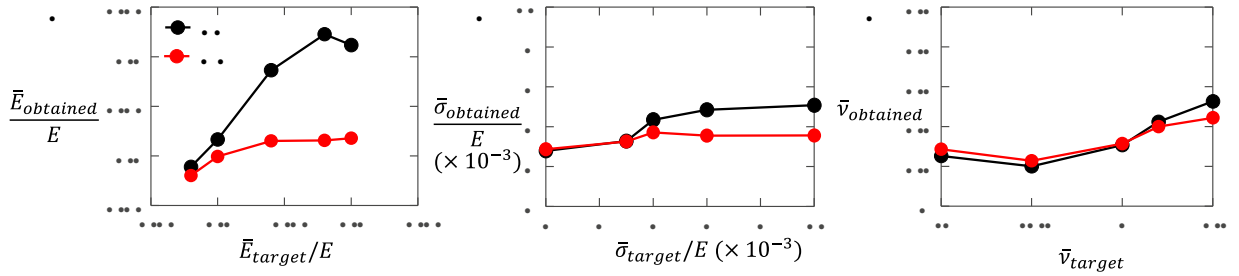

Figure 5 Comparison between GA predicted mechanical properties—(A) nondimensional effective stiffness, (B) nondimensional effective critical strength, and (C) effective Poisson's ratio—and FE simulated results

The comparison between the initial and final ranges—the value of range were corrected by FE simulations—are summarized in Table 1. These results show the significant enhancement of design space, which obtained by our constructed inverse design algorithm driven by GNN.

Table 1: Comparison between initial and final design space of nonuniform triangular lattice structures

	$\bar{E}/E$	$\bar{\sigma}_{cr}/E$	$\bar{\nu}$
Initial range	[0.11, 0.19]	[0.019, 0.0032]	[0.075, 0.237]
Final range	[0.049, 0.32]	[0.0006, 0.0052]	[-0.12, 0.28]

4. Conclusions

In this study, GNN-GA driven inverse design algorithm that can create new nonuniform triangular lattice structures with target mechanical properties is developed. Initially, 10,000 datasets were randomly selected to build training, validation and testing datasets. The GNN was then trained to achieve best prediction performance as a surrogate model in the inverse design algorithm. Subsequently, GA was implemented as global searching algorithm to successfully optimize the design of nonuniform triangular lattice structures with target properties—nondimensional effective stiffness, nondimensional effective critical strength and effective Poisson's ratio. These findings provide promising approach to design complex nonuniform lattice structures.

Acknowledgements

The authors acknowledge the partially support from MSCA DN GAP project (No. 101120290).

References

Benedetti, M., du Plessis, A., Ritchie, R. O., Dallago, M., Razavi, N., & Berto, F. (2021). Architected cellular materials: A review on their mechanical properties towards fatigue-tolerant design and fabrication. Materials Science and Engineering: R: Reports, 144, 100606.

Fey, M., & Lenssen, J. E. (2019). Fast Graph Representation Learning with PyTorch Geometric. arXiv:1903.02428.

Gu, G. X., Chen, C.-T., Richmond, D. J., & Buehler, M. J. (2018). Bioinspired hierarchical composite design using machine learning: simulation, additive manufacturing, and experiment. Materials Horizons, 5(5), 939-945.

Ha, C. S., Lakes, R. S., & Plesha, M. E. (2019). Cubic negative stiffness lattice structure for energy absorption: Numerical and experimental studies. International Journal of Solids and Structures, 178-179, 127-135.

Harris, C. R., Millman, K. J., van der Walt, S. J., Gommers, R., Virtanen, P., Cournapeau, D., Wieser, E., Taylor, J., Berg, S., Smith, N. J., Kern, R. Picus, M., Hoyer, S., van Kerkwijk, M. H., Brett, M., Haldane, A., del Rio, J. F., Wiebe, M., Peterson, P., Gerard-Marchant, P., Sheppard, K., Reddy, T., Weckesser, W., Abbasi, H., Gohlke, C., Oliphant, T. E. (2020). Array programming with NumPy. Nature, 585(7825), 357-362.

Jiang, B., Wang, Y., Niu, H., Cheng, X., Zhao, P., & Bao, J. (2024). GNNs for mechanical properties prediction of strut-based lattice structures. International Journal of Mechanical Sciences, 269, 109082.

Maurizi, M., Gao, C., & Berto, F. (2022a). Inverse design of truss lattice materials with superior buckling resistance. npj Computational Materials, 8(1), 247.

Maurizi, M., Gao, C., & Berto, F. (2022b). Predicting stress, strain and deformation fields in materials and structures with graph neural networks. Scientific Reports, 12(1), 21834.

Michalewicz, Z., & Schoenauer, M. (1996). Evolutionary Algorithms for Constrained Parameter Optimization Problems. Evolutionary Computation, 4(1), 1-32.

Murr, L. E., Gaytan, S. M., Medina, F., Lopez, H., Martinez, E., Machado, B. I., Hernandez, D. H., Martinez, L., Lopez, M. I., Wicker, R. B., Bracke, J. (2010). Next-generation biomedical implants using additive manufacturing of complex, cellular and functional mesh arrays. Philosophical Transactions of the Royal Society A: Mathematical, Physical and Engineering Sciences, 368(1917), 1999-2032.

Najmon, J. C., DeHart, J., Wood, Z., & Tovar, A. (2018). Cellular Helmet Liner Design through Bio-inspired Structures and Topology Optimization of Compliant Mechanism Lattices. SAE International Journal of Transportation Safety, 6(3), 217-235.

Pan, C., Han, Y., & Lu, J. (2020). Design and Optimization of Lattice Structures: A Review. Applied Sciences, 10(18), 6374.

Paszke, A., Gross, S., Massa, F., Lerer, A., Bradbury, J., Chanan, G., Killeen, T., Lin, Z., Gimelsheim, N., Antiga, L., Desmaison, A., Kopf, A., Yang, E., DeVito, Z., Raison, M., Tejani, A., Chilamkurthy, S., Steiner, B., Fang, L., Bai, J., chintala, S. (2019). PyTorch: An Imperative Style, High-Performance Deep Learning Library. arXiv:1912.01703.

Roberts, A. P., & Garboczi, E. J. (2002). Elastic properties of model random three-dimensional open-cell solids. Journal of the Mechanics and Physics of Solids, 50(1), 33-55.

Schaedler, T. A., Jacobsen, A. J., Torrents, A., Sorensen, A. E., Lian, J., Greer, J. R., Valdevit, L., Carter, W. B. (2011). Ultralight Metallic Microlattices. Science, 334(6058), 962-965.

Sunder Sharma, S., Yadav, S., Joshi, A., Goyal, A., & Khatri, R. (2022). Application of metallic foam in vehicle structure: A review. Materials Today: Proceedings, 63, 347-353.

Veličković, P., Cucurull, G., Casanova, A., Romero, A., Liò, P., & Bengio, Y. (2017). Graph Attention Networks. arXiv:1710.10903.

Wadley, H. N. G., & Queheillalt, D. T. (2007). Thermal Applications of Cellular Lattice Structures. Materials Science Forum, 539-543, 242-247.

Xue, X., Lin, C., Wu, F., Li, Z., & Liao, J. (2023). Lattice structures with negative Poisson's ratio: A review. Materials Today Communications, 34, 105132.